Biochemical and Biophysical Research Communications 443 (2014) 658–665

Contents lists available at ScienceDirect

Biochemical and Biophysical Research Communications

journal homepage: www.elsevier.com/locate/ybbrc

Dioscin inhibits osteoclast differentiation and bone resorption though down-regulating the Akt signaling cascades

Xinhua Qu [a,1], Zanjing Zhai [a,1], Xuqiang Liu [a,1], Haowei Li [a], Zhengxiao Ouyang [a,b], Chuanlong Wu [a], Guangwang Liu [c], Qiming Fan [a], Tingting Tang [a], An Qin [a,*], Kerong Dai [a,*]

[a] Shanghai Key Laboratory of Orthopaedic Implants, Department of Orthopaedics, Ninth People's Hospital, Shanghai Jiao Tong University School of Medicine, Shanghai, China
[b] Department of Orthopaedics, Hunan Provincial Tumor Hospital and Tumor Hospital of Xiangya School of Medicine, Central South University, Changsha, China
[c] Department of Orthopaedic Surgery, The Central Hospital of Xuzhou, Affiliated Hospital of Medical Collage of Southeast University, Xuzhou, China

ARTICLE INFO

Article history:
Received 28 November 2013
Available online 11 December 2013

Keywords:
Dioscin
Osteoclast
Osteolysis
AKT cascades

ABSTRACT

Bone resorption is the unique function of osteoclasts (OCs) and is critical for both bone homeostasis and pathologic bone diseases including osteoporosis, rheumatoid arthritis and tumor bone metastasis. Thus, searching for natural compounds that may suppress osteoclast formation and/or function is promising for the treatment of osteoclast-related diseases. In this study, we for the first time demonstrated that dioscin suppressed RANKL-mediated osteoclast differentiation and bone resorption *in vitro* in a dose-dependent manner. The suppressive effect of dioscin is supported by the reduced expression of osteoclast-specific markers. Further molecular analysis revealed that dioscin abrogated AKT phosphorylation, which subsequently impaired RANKL-induced nuclear factor-kappaB (NF-κB) signaling pathway and inhibited NFATc1 transcriptional activity. Moreover, *in vivo* studies further verified the bone protection activity of dioscin in osteolytic animal model. Together our data demonstrate that dioscin suppressed RANKL-induced osteoclast formation and function through Akt signaling cascades. Therefore, dioscin is a potential natural agent for the treatment of osteoclast-related diseases.

1. Introduction

Bone is a rigid yet dynamic organ that is continuously shaped and repaired [1]. The delicate balance between osteoblastic bone formation and osteoclastic bone resorption is necessary for bone metabolic homeostasis. Excessive osteoclast formation and bone resorption can cause adult skeletal diseases including osteoporosis, rheumatoid arthritis, multiple myeloma and tumor bone metastasis [2].

The formation of functional osteoclasts requires two key molecules, monocyte/macrophage-colony stimulating factor (M-CSF) and the receptor activator of nuclear factor κB (NF-κB) ligand (RANKL) [3]. RANKL is crucial for osteoclast function by binding to its receptor RANK and thereby activating downstream signaling cascades including the NF-κB pathway, Src/phosphatidylinositide (PI) 3-kinase/Akt axis, mitogen activated protein kinases (MAPK) signaling pathway and so on[4]. Previous literatures demonstrated blockage of key RANKL signalings are potential for the treatment of osteoclast-related diseases.

Dioscin is a natural product derived from medicinal plants such as Dioscorea nipponica Makino and Dioscorea zingiberensis Wright [5,6]. Pharmacological researches have demonstrated that dioscin has anti-inflammatory, lipid-lowering, anti-tumor and hepatoprotective properties [7–9]. It has also been widely used as an important raw material for the synthesis of steroid hormone drugs such as cortisone [10]. However, to the best of our knowledge, the effects of dioscin on bone biology is yet unknown. Therefore, this study aims to investigate the pharmacological effects of dioscin on osteoclast *in vitro* and *in vivo*.

2. Materials and methods

2.1. Media and reagents

Dioscin was purchased from Sigma–Aldrich (St. Louis, MO, USA). Alpha-MEM, foetal bovine serum (FBS), and penicillin were purchased from Gibco BRL (Gaithersburg, MD, USA). Soluble mouse recombinant M-CSF and RANKL were purchased from R&D Systems (USA). Tartrate-resistant acid phosphatase (TRAP) staining solution was from Sigma–Aldrich. The Cell Counting Kit-8 (CCK-8) was obtained from Dojindo Molecular Technology (Japan). Primary antibodies targeting β-actin, phospho-IκBα, IκBα, phospho-AKT,

* Corresponding authors. Fax: 86 21 63139920.
E-mail addresses: dr.qinan@gmail.com (A. Qin), krdai@163.com (K. Dai).
[1] These authors contributed equally to this work.

0006-291X/$ - see front matter © 2013 Elsevier Inc. All rights reserved.
http://dx.doi.org/10.1016/j.bbrc.2013.12.029

AKT, phospho-ERK, ERK, phospho-JNK, JNK, phospho-p38, p38 and NFATc1 were purchased from Cell Signaling Technology (CST, Danvers, MA, USA).

2.2. Cell viability assay

The anti-proliferative effect of dioscin on BMMs cells was assessed with a cell counting kit-8 (CCK-8, Dojindo Laboratories, Kumamoto, Japan). Briefly, after treatment, 10 μl CCK-8 solution was added to each well; after 4 h incubation, absorbance was measured at 450 nm using a microplate reader. The effect of dioscin on cell viability was expressed as percent cell viability with vehicle-treated control cells set at 100%.

2.3. In vitro osteoclastogenesis assay

In vitro osteoclastogenesis assays were preformed to examine the effects of dioscin on osteoclast differentiation. Bone marrow macrophages (BMM) cells were prepared as previously described [11–14]. Briefly, cells extracted from the femur and tibiae of a 6-week-old C57/BL6 mouse were incubated in complete cell culture media and 30 ng/mL M-CSF in a T-75 cm^2 flask for proliferation. When changing the medium, the cells were washed in order to deplete residual stromal cells. After reaching 90% confluence, cells were washed with phosphate-buffered saline (PBS) three times and trypsinised for 30 min to harvest BMMs. Adherent cells on dish bottoms were classified as BMMs; these BMMs were plated in the 96-well plates at a density of 8×10^3 cells/well in triplicate and incubated in a humidified incubator containing 5% CO_2 at 37 °C for 24 h. The cells were then treated with various concentrations of dioscin (0, 1, or 4 μM) plus M-CSF (30 ng/mL) and RANKL (50 ng/mL). After five days, cells were fixed and stained for TRAP activity. TRAP+ multinucleated cells with more than five nuclei were counted as osteoclasts.

2.4. Resorption pit assay

For the bone resorption assay were carried out as previously described [15,16], BMMs were seeded on bone slices in 96-well plates at a density of 8×10^3 cells/well with three replicates and stimulated with M-CSF (30 ng/mL) plus RANKL (50 ng/mL). Three days later, cells were treated with the indicated concentrations of dioscin for 48 h post-culture. Cells were then fixed with 2.5% glutaraldehyde. Bone slices were imaged using a scanning electron microscope (SEM; FEI Quanta 250) with 200× magnification and at 10 kV. Three view fields were randomly selected for each bone slice for further analysis. Pit areas were quantified using Image J software (National Institutes of Health). Similar independent experiments were repeated for at least three times.

2.5. Western blot analysis

BMMS cells were seeded at 5×10^5 cells/well into 6-well plates and pretreated with or without dioscin (4 μM) for 4 h prior to RANKL stimulation (50 ng/mL) for the indicated times (0, 5, 15 or 30 min). BMMs were seeded at 5×10^5 cells/well into 6-well plates and treated with or without dioscin (4 μM) and RANKL (50 ng/mL) for the indicated times. Cells were lysed in RIPA lysis buffer containing 50 mM Tris–HCl, 150 mM NaCl, 5 mM EDTA, 1% Triton X-100, 1 mM sodium fluoride, 1 mM sodium vanadate, 1% deoxycholate, and protease inhibitor cocktail. The lysate was centrifuged at 12,000 rcf for 10 min, and the protein in the supernatant was collected. Protein concentrations were measured though BCA assay. Thirty micrograms of each protein lysate was resolved by sodium dodecyl sulfate–polyacrylamide gel electrophoresis (SDS–PAGE) using 8–10% gels, and proteins were then transferred to polyvinylidene difluoride membranes (Millipore, Bedford, MA, USA). Nonspecific interactions were blocked with 5% skim milk for 1 h, and membranes were then probed with the indicated primary antibodies overnight at 4 °C as indicated. Membranes were incubated with the appropriate secondary antibodies conjugated with IRDye 800CW (molecular weight, 1166 Da), and the antibody reactivity was detected by exposure in an Odyssey infrared imaging system (Li-COR).

2.6. Luciferase reporter gene activity assay

The effects of dioscin on RANKL-induced NF-κB activation were measured using RAW264.7 cells that had been stably transfected with an NF-κB luciferase reporter construct, as previously described [14,17]. Briefly, cells were seeded into 48-well plates and maintained in cell culture media for 24 h. Cells were then pretreated with or without the indicated concentrations of dioscin for 1 h, followed by addition of RANKL (50 ng/mL) for 8 h. Luciferase activity was measured using the Promega Luciferase Assay System (Promega, Madison, WI, USA) and normalised to that of the vehicle control. Similarly, the effect of dioscin on RANKL-induced AP-1- or NFATc1-dependent luciferase reporter assays was determined as described previously [18,19].

2.7. Quantitative PCR analysis

For real-time PCR, 10×10^4 BMMs were seeded in each well of a 24-well plate and cultured in complete medium containing α-MEM, 10% FBS, 100 U/mL penicillin, M-CSF (30 ng/mL), and RANKL (50 ng/mL). Cells were then treated with or without dioscin (4 μM) for the indicated times. Total RNA was prepared using an RNeasy Mini kit (Qiagen, Valencia, CA, USA) according to the manufacturer's instructions, and cDNA was synthesised from 1 μg of total RNA using reverse transcriptase (TaKaRa Biotechnology, Otsu, Japan). Real-time PCR was performed using the SYBR Premix Ex Tag kit (TaKaRa Biotechnology) and an ABI 7500 Sequencing Detection System (Applied Biosystems, Foster City, CA, USA). The detector was programmed with the following PCR conditions: 40 cycles for 5 s denaturation at 95 °C and 34 s amplification at 60 °C. All reactions were run in triplicate and were normalised to the housekeeping gene β-actin. The following primer sets were used as previously described [20,21]: mouse β-actin: forward, 5′-TCT GCTGGAAGGTGGACAGT-3′ and reverse, 5′-CCTCTATGCCAACA CAGTGC-3′; mouse NFATc1: forward, 5′-CCGTTGCTTCCAGAAAATA ACA-3′ and reverse, 5′-TGTGGGATGTGAACTCGGAA-3′; mouse TRAP: forward, 5′-CTGGAGTGCACGATGCCAGCGACA-3′ and reverse, 5′-TCCGTGCTCGGCGATGGACCAGA-3′; mouse cathepsin K: forward, 5′-CTTCCAATACGTGCAGCAGA-3′ and reverse, 5′-TCTTCA GGGCTTTCTCGTTC-3′; mouse CTR: forward, 5′-TGCAGACAACT CTTGGTTGG-3′ and reverse, 5′-TCGGTTTCTTCTCCTCTGGA-3′.

2.8. In vivo experiments

The Animal Care and Experiment Committee of Shanghai Jiao Tong University School of Medicine approved all experimental procedures, and the study was carried out according to the guidelines for Ethical Conduct in the Care and Use of Nonhuman Animals in Research by the American Psychological Association. Mice were injected intraperitoneally dioscin (5 mg/kg body weight) or PBS as control 1 day before injection of LPS (5 μg/g body weight). dioscin or PBS was injected intraperitoneally every other day for 8 days. LPS was injected intraperitoneally on days 1 and 4. All mice were sacrificed 8 days after the initial LPS injection and the femurs were dissected and fixed in 4% paraformaldehyde (Sigma–Aldrich, St. Louis, MO) for 1 day at 4 °C and were then decalcified in 12% EDTA. Decalcified bones were paraffin-embedded and sectioned. For

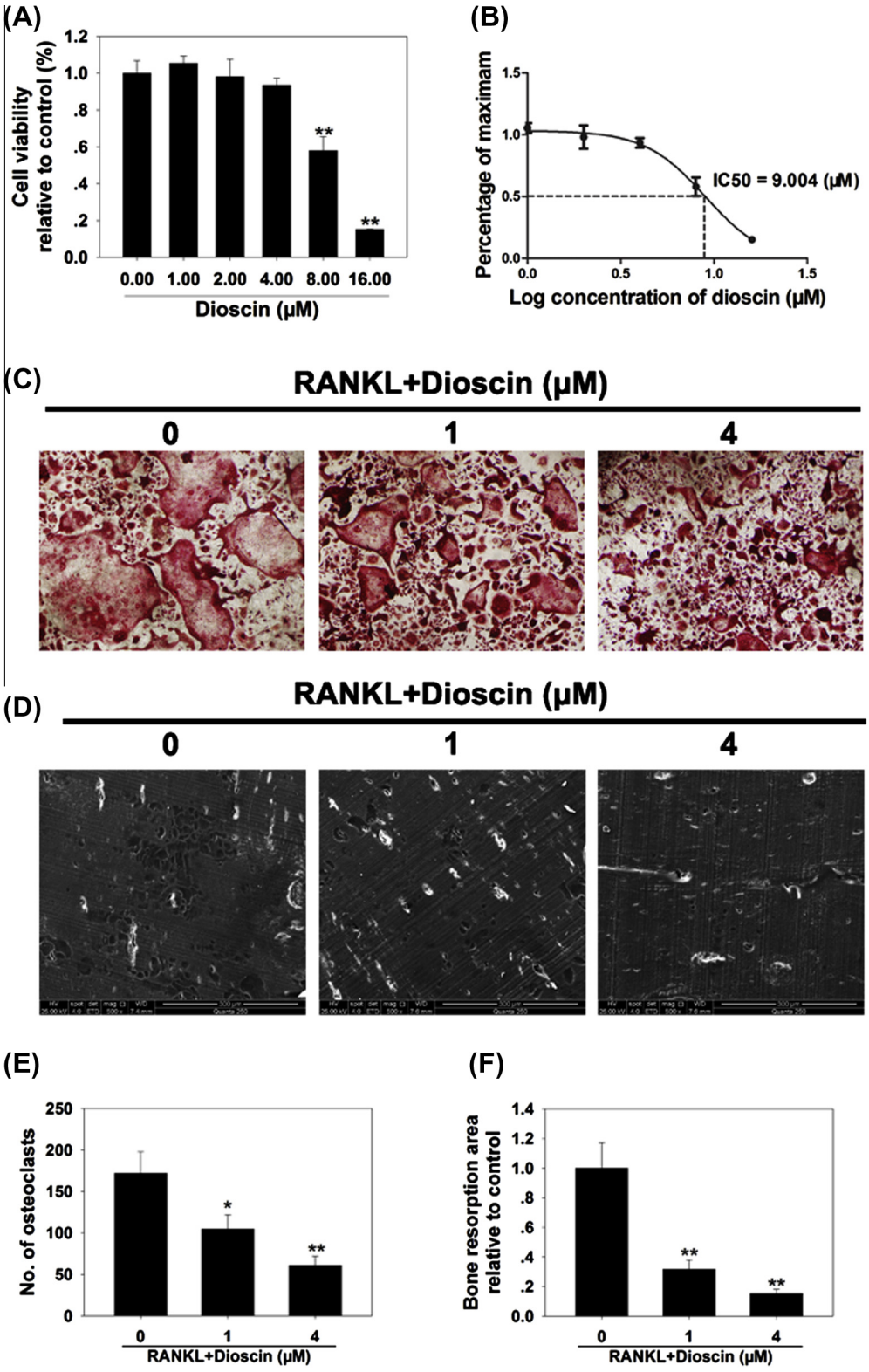

Fig. 1. Dioscin inhibited RANKL-induced osteoclast formation and bone resorption in a concentration-dependent manner without any cytotoxicity. (A) Viability of dioscin-treated BMMs cells. (B) The half-maximal inhibitory concentration (IC_{50}) of dioscin was 9.004 μM. (C) Bone marrow-derived monocytes/macrophages (BMMs) were treated with various concentrations of dioscin followed by M-CSF (30 ng/mL) and RANKL (50 ng/mL) stimulation for five days. Cells were then fixed with 4% PFA and subjected to TRAP staining. (D) BMM-derived pre-osteoclasts were stimulated with M-CSF (30 ng/mL) and RANKL (50 ng/mL for three days. Later, cells were cultured in the presence of the indicated concentrations of dioscin with M-CSF (30 ng/mL) and RANKL (50 ng/mL) for another 48 h. SEM images of bone resorption pits are shown. (E) TRAP-positive multinuclear cells were counted. (F) Resorption pit areas were measured using Image J and are presented graphically. All experiments were carried out at least three times, and the significance was determined by Student–Newman–Keul's tests ($^{*}P < 0.05$; $^{**}P < 0.01$).

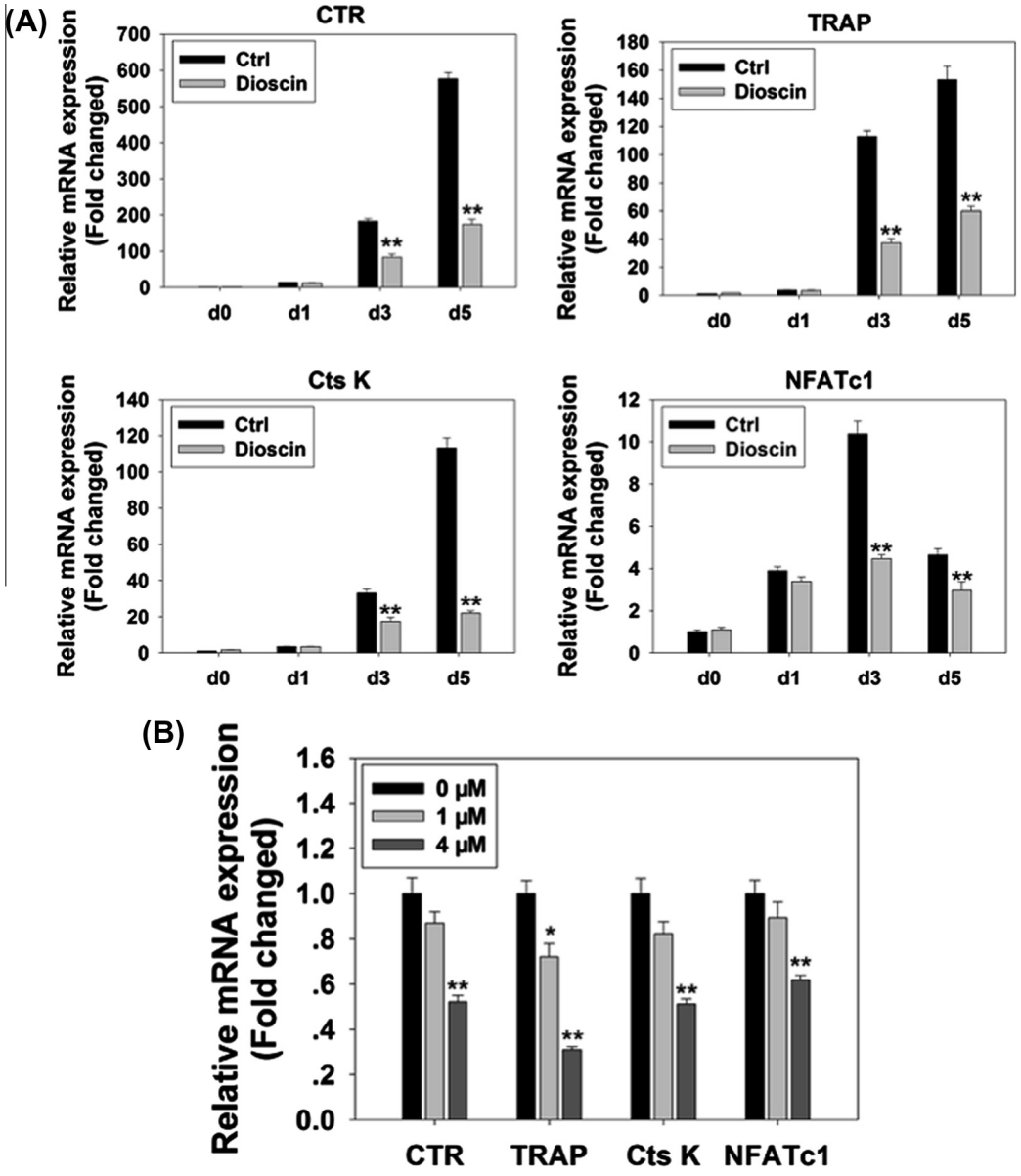

Fig. 2. Dioscin suppressed RANKL-induced expression of osteoclast-specific genes. (A) BMMs were cultured with M-CSF (30 ng/mL) and RANKL (50 ng/mL), with or without 4 μM dioscin, for 0, 1, 3, or 5 days. Osteoclast-specific gene expression (*TRAP*, *CTR*, *Cts k*, and *NFATc1*) was analysed by real-time PCR, and results were normalised to the expression of β-actin. (B) BMMs were cultured with M-CSF (30 ng/mL) and RANKL (50 ng/mL), with indicated concentrations of dioscin for 5 days. Osteoclast-specific gene expression (*TRAP*, *CTR*, *Cts k*, and *NFATc1*) was analysed by real-time PCR, and results were normalised to the expression of β-actin. All experiments were performed at least three times ($^{*}P < 0.05$; $^{**}P < 0.01$).

histologic examination, sections were stained with hematoxylin and eosin (H&E), and another section was stained with TRAP to identify osteoclasts on the bone surface. Parameters for the percentage osteoclast surface per bone surface (OcS/BS, %), number of osteoclasts per field of tissue, as well as the microstructural indices of trabecular bone density (BV/TV), trabecular thickness (Tb.Th), trabecular number (Tb.N), and trabecular space (Tb.Sp) were measured to assess the trabecular bone microstructure of the femurs were quantified by using the Image Pro-Plus program, version 4.0 (Media Cybernetics, Silver Spring, MD).

2.9. Statistical analysis

All values are presented as the mean ± standard deviation (S.D.) of the values obtained from three or more experiments. Statistical significances were determined by Student's *t*-test. A value of $P < 0.05$ was considered significant.

3. Results

3.1. Dioscin does not inhibit BMMs proliferation at low concentrations

After 48-h culture, a CCK-8 proliferation assay showed that dioscin did not affect BMMs cell proliferation at concentrations 4 μM (Fig. 1A). Dioscin partially suppressed cell proliferation at concentrations ⩾8 μM. The calculated IC_{50} for dioscin was 9.004 μM (Fig. 1B). In order to exclude dioscin-mediated cytotoxicity, non-lethal concentrations (⩽4 μM) were used in subsequent experiments.

3.2. Dioscin inhibits RANKL-induced osteoclast formation and bone resorption in vitro

To investigate the effects of dioscin on osteoclastogenesis, BMMs were treated with various concentrations of dioscin during the course of osteoclast formation. As shown in Fig. 1C, the control

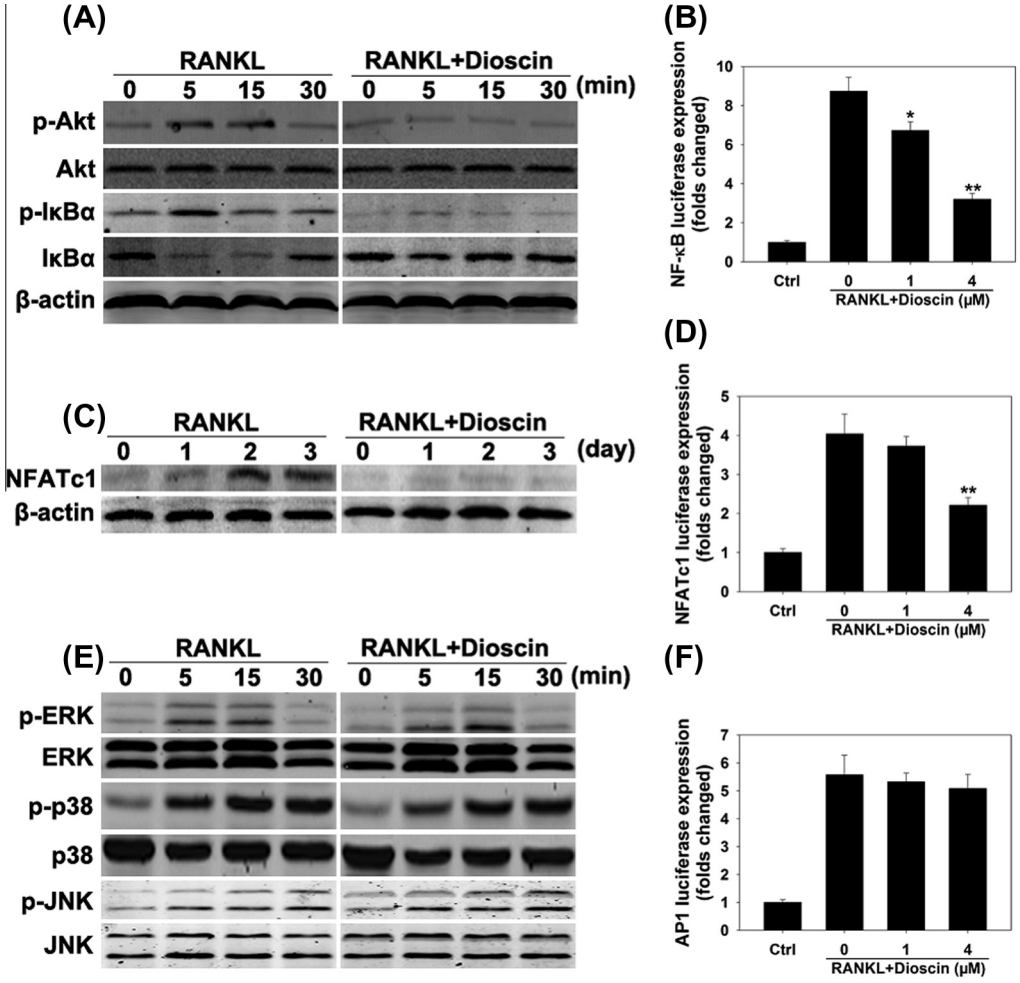

Fig. 3. Dioscin inhibited RANKL-induced activation of NF-κB/NFATc1 and AKT signaling pathways. (A) RAW264.7 cells were seeded at 5×10^5 cells/well in 6-well plates and pretreated with or without dioscin (4 μM) for 4 h prior to RANKL stimulation (50 ng/mL) for the indicated times. Cells were lysed for Western blotting with specific antibodies against phospho-IκBα, IκBα, phospho-AKT, AKT and actin. (B) Stably transfected RAW264.7 cells with an NF-κB luciferase reporter construct were seeded in 48-well plates and maintained in the cell culture media for 24 h. The cells were then pretreated with or without the indicated concentrations of dioscin for 1 h, followed by addition of RANKL (50 ng/mL) for 8 h. NF-κB luciferase activity was measured. (C) RAW264.7 cells were seeded at 5×10^5 cells/well in 6-well plates and treated with or without dioscin (4 μM) for the indicated days. Cells were lysed for Western blotting with specific antibodies against NFATc1 and actin. (D) Stably transfected RAW264.7 cells with an NFATc1 luciferase reporter construct were seeded in 48-well plates and maintained in the cell culture media for 24 h. The cells were then pretreated with or without the indicated concentrations of dioscin for 1 h, followed by addition of RANKL (50 ng/mL) for 24 h. NFATc1 luciferase activity was measured. (E) RAW264.7 cells were seeded at 5×10^5 cells/well in 6-well plates and pretreated with or without dioscin (4 μM) for 4 h prior to RANKL stimulation (50 ng/mL) for the indicated times. Cells were lysed for Western blotting with specific antibodies against phospho-ERK, ERK, phospho-JNK, JNK, phospho-p38 and p38. (F) Stably transfected RAW264.7 cells with an AP-1 luciferase reporter construct were seeded in 48-well plates and maintained in the cell culture media for 24 h. The cells were then pretreated with or without the indicated concentrations of dioscin for 1 h, followed by addition of RANKL (50 ng/mL) for 24 h. AP-1 luciferase activity was measured. All experiments were performed at least three times ($^*P < 0.05$; $^{**}P < 0.01$).

group formed numerous TRAP-positive multinucleated osteoclasts. In contrast, the formation of osteoclasts was inhibited after dioscin treatment, especially at the 4 μM concentration (Fig. 1C). This is further supported by statistical analysis of the number of osteoclasts formed, where the control group formed 172 ± 26.8 osteoclasts per well, but only 61 ± 11.3 osteoclasts per well in the 4 μM concentration group (Fig. 1E).

Since dioscin inhibited osteoclast formation, we next investigated whether dioscin could impair osteoclastic bone resorption *in vitro*. As shown in Fig. 1D, dioscin treatment substantially reduced osteoclastic bone resorption area. Osteoclastic bone resorption was almost completely abrogated after being treated with 4 μM dioscin (Fig. 1F). Collectively, these findings suggested that dioscin impaired osteoclast formation and bone resorption *in vitro*.

3.3. Dioscin suppressed osteoclastic gene expression in vitro

To further confirm the inhibitory effect of dioscin on osteoclast differentiation, osteoclastic gene expression profile was investigated by realtime PCR. As shown in Fig. 2A, the expression of osteoclastic specific genes was gradually induced during osteoclastogenesis, including TRAP, CtsK and CTR. What's more, NFATc1 reached its peak at the mid-phrase of osteoclast differentiation. However, the induction of these genes was suppressed dramatically by the presence of dioscin. In addition, dioscin dose-dependently suppressed these osteoclast specific genes (TRAP, Cts K, CTR, and NFATc1) at 1 and 4 μM respectively (Fig. 2B). Collectively, these data supported the inhibition of osteoclast formation by dioscin.

3.4. Dioscin inhibited the RANKL-induced AKT/NF-κB and AKT / NFATc1activation

To further elucidate the mechanisms through which dioscin suppressed osteoclast formation, RANKL-induced signaling pathways were investigated. Here, we found the phosphorylation of Akt was significantly inhibited by dioscin (Fig. 3A). Since Akt is important for both Akt/NF-κB and Akt/NFATc1 cascades, we thus

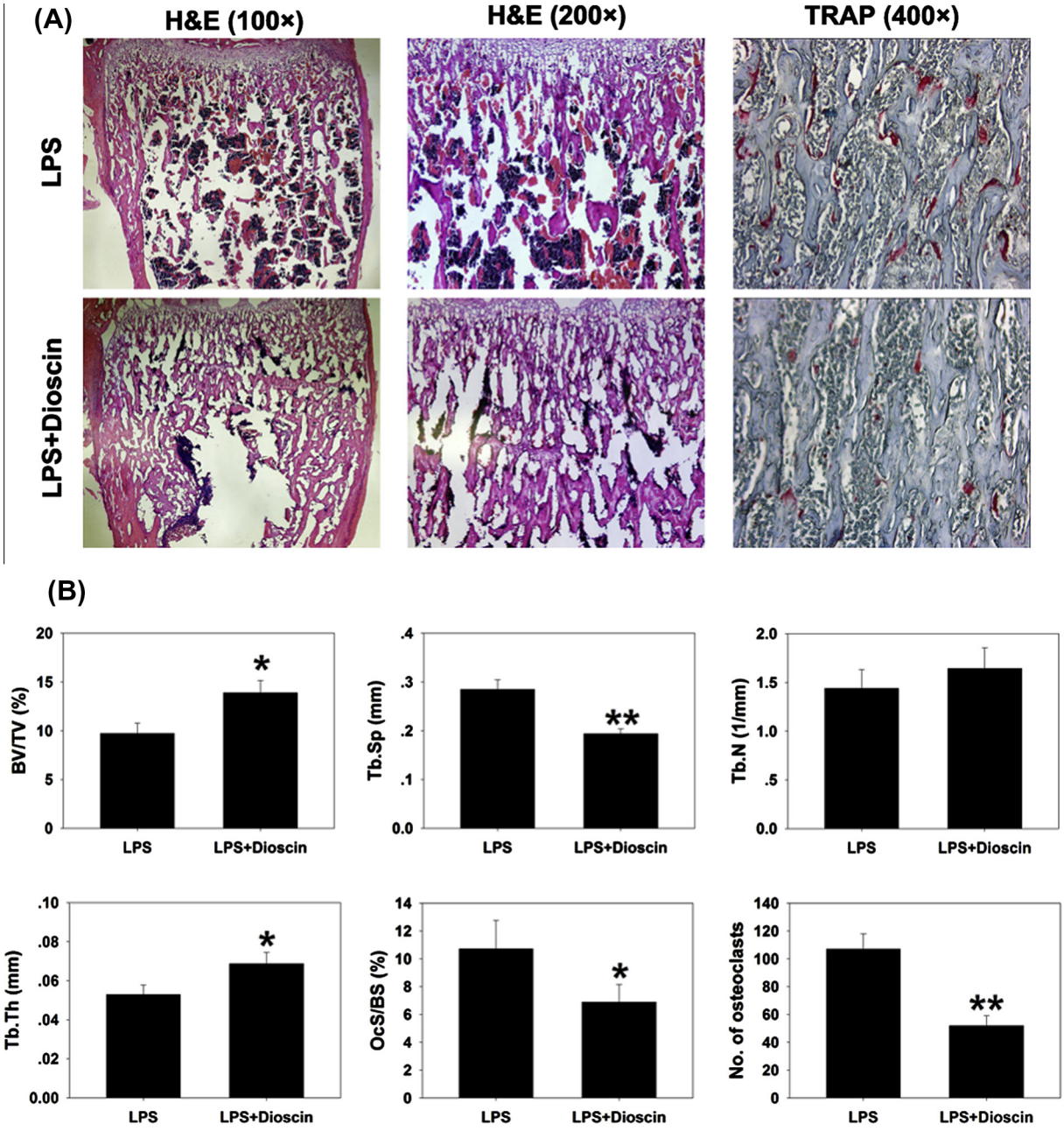

Fig. 4. Dioscin prevented LPS-induced bone loss by inhibiting osteoclast activity. (A) Femurs were fixed, decalcified, dehydrated, embedded, and sectioned. Sections were stained with H&E (100× and 200×) and TRAP (400×). (B) Percentage osteoclast surface per bone surface (OcS/BS, %), and (C) number of osteoclasts per field of tissue (No. of OCs/field) in 400× magnification were analysed. Asterisks indicate statistically significant differences ($^{*}P < 0.05$; $^{**}P < 0.01$) between groups.

further investigated these two key signaling pathways during osteoclast differentiation. As shown in Fig. 3A, RANKL-induced IκBα phosphorylation and degradation was markedly suppressed by dioscin. More specifically, IκBα was phosphorylated and degraded upon RANKL stimulation for 5 min in the control group. In contrast, dioscin treatment suppressed the phosphorylation and therefore degradation of IκBα (Fig. 3A). This was further evidenced by luciferase assay that dioscin blocked of NF-κB activation in a concentration-dependent manner (Fig. 3B).

Akt is also known to regulate osteoclast differentiation by regulating Akt/NFATc1 signaling pathway [22]. Therefore, we further checked the expression of NFATc1 after dioscin treatment. Here, our Western blot analysis demonstrated that RANKL induced NFATc1 expression during osteoclast formation. However, the expression of NFATc1 was significantly suppressed after dioscin treatment (Fig. 3C). This was in consistent with our real-time PCR results, which demonstrated the suppression of NFATc1 mRNA after dioscin treatment (Fig. 2). Luciferase analysis results of declined transcriptional activity further demonstrated dioscin's inhibitory effect on NFATc1 (Fig. 3D).

In addition, we also investigated other key signaling pathways involved in osteoclast differentiation [23–25]. We examined the phosphorylation of p38, JNK and ERK and showed that dioscin had no obvious effect on these signaling pathways (Fig. 3E). Furthermore, we also demonstrated that dioscin does not affect AP-1 activity by AP-1 luciferase reporter gene assays.

Together, these results revealed that dioscin specifically inhibited the Akt/NF-κB and Akt/NFATc1 activation during osteoclast differentiation without affecting MAPK/AP-1 pathways.

3.5. Dioscin prevented bone destruction induced by LPS in vivo

To address the effect of dioscin *in vivo*, osteolytic mouse model was chosen by LPS injection as previously described in our group [14]. Mice were intraperitoneally injected with LPS with or without dioscin. No fatalities were recorded after LPS and dioscin administration, and the animals retained normal activity throughout the duration of the experiment. Histological examination confirmed the protective effects of dioscin on LPS-induced bone loss. As shown in Fig. 4A, RANKL injection led to bone erosion and increased numbers of TRAP-positive osteoclasts. However, bone erosion was rescued in dioscin-treated mouse femur tissue sections, which was consistent with decreased TRAP-positive osteoclasts (Fig. 4A). Furthermore, histomorphometric analysis of OcS/BS and No. of OCs demonstrated that dioscin reduced LPS-activated osteoclast numbers, and microstructural indices of BV/TV, Tb.Th, and Tb.Sp further identified dioscin protective effect in inflammatory bone loss, even though no significantly increased Tb.N was witnessed (Fig. 4B). Taken together, our data indicated that dioscin prevented LPS-induced bone loss *in vivo*.

4. Discussion

In this study, we have verified for the first time that natural compound dioscin inhibited osteoclast differentiation and bone resorption, suggesting an additional protective effect of dioscin on osteoclast-related diseases. In addition, we revealed the molecular mechanisms of dioscin on osteoclasts are through suppressing Akt/NF-κB and Akt/NFATc1 signaling pathways.

In osteoclasts, the Akt signaling cascades is a critical downstream of three osteoclast surface receptors including c-fms, αvβ3 integrin and RANK [22,26]. Previous studies demonstrated Akt phosphorylation is activated upon both M-CSF and RANKL stimulation and play critical roles in osteoclastogenesis by affecting both NF-κB and NFATc1 activation. Moon et al. demonstrated that overexpression of Akt in BMMs strongly induced NFATc1 expression and lead to enhanced osteoclastogenesis [22]. Besides, activation of NF-κB can be initiated by several different kinases such as Akt and NF-κB inducing kinase. Gingery et al. demonstrated that AKT/NF-κB axis is critical in osteoclastogenesis and maintaining mature osteoclast survival [27,28]. In consistent with these studies, we demonstrated that dioscin inhibited Akt phosphorylation and thus suppressed the RANKL-induced NF-κB activity and NFATc1 activity, both of which are critical for osteoclast differentiation. Interestingly, in the process of detecting the function of dioscin on MAPKs pathway, no significantly inhibitory impact was witnessed.

In summary, dioscin is capable of inhibiting osteoclast formation and function, indicating additional therapeutic benefits of dioscin for osteoclast-related diseases. In addition, this study also clearly revealed the molecular mechanisms of dioscin on osteoclasts are via impairing Akt/NF-κB and Akt/NFATc1 signaling pathways *in vitro*. In addition, our *in vitro* results further verified the bone protective role of dioscin on LPS-induced osteolysis model. However, further investigation of dioscin on other cells within bone is still required.

Conflict of interest

No authors have any conflicts of interest to declare.

Acknowledgments

This work was supported by the Program for Innovative Research Team of Shanghai Municipal Education Commission (Phase I), a Grant awarded for Innovative Research from Shanghai Municipal Education Commission (13YZ031), a Grant awarded by the Key Disciplines of Shanghai Municipal Education Commission of China (J50206), a Grant for scientific research from the National Natural Science Foundation for the Youth of China (No. 81201364), and a Grant awarded by the Scientific Research Foundation for Returned Overseas Chinese Scholars from the State Human Resource Ministry.

References

[1] S.L. Teitelbaum, Bone resorption by osteoclasts, Science 289 (2000) 1504–1508.
[2] Y. Tanaka, S. Nakayamada, Y. Okada, Osteoblasts and osteoclasts in bone remodeling and inflammation, Curr. Drug Targets: Inflammation Allergy 4 (2005) 325–328.
[3] T. Suda, N. Takahashi, N. Udagawa, E. Jimi, M.T. Gillespie, T.J. Martin, Modulation of osteoclast differentiation and function by the new members of the tumor necrosis factor receptor and ligand families, Endocr. Rev. 20 (1999) 345–357.
[4] Z.H. Lee, H.-H. Kim, Signal transduction by receptor activator of nuclear factor kappa B in osteoclasts, Biochem. Biophys. Res. Commun. 305 (2003) 211–214.
[5] T. Nakamura, C. Komori, Y.-Y. Lee, F. Hashimoto, S. Yahara, T. Nohara, A. Ejima, Cytotoxic activities of Solanum steroidal glycosides, Biol. Pharm. Bull. 19 (1996) 564–566.
[6] X. Wang, The expanding role of mitochondria in apoptosis, Genes Dev. 15 (2001) 2922–2933.
[7] Y. Wang, C.-M. Che, J.-F. Chiu, Q.-Y. He, Dioscin (saponin)-induced generation of reactive oxygen species through mitochondria dysfunction: a proteomic-based study, J. Proteome Res. 6 (2007) 4703–4710.
[8] M. Sautour, A.-C. Mitaine-Offer, T. Miyamoto, A. Dongmo, M.-A. Lacaille-Dubois, Antifungal steroid saponins from Dioscorea cayenensis, Planta Med. 70 (2004) 90–92.
[9] M.J. Kaskiw, M.L. Tassotto, M. Mok, S.L. Tokar, R. Pycko, J. Th'ng, Z.-H. Jiang, Structural analogues of diosgenyl saponins: synthesis and anticancer activity, Bioorg. Med. Chem. 17 (2009) 7670–7679.
[10] N. Brautbar, J. Williams II, Industrial solvents and liver toxicity: risk assessment, risk factors and mechanisms, Int. J. Hyg. Environ. Health 205 (2002) 479–491.
[11] A. Qin, T.S. Cheng, Z. Lin, L. Cao, S.M. Chim, N.J. Pavlos, J. Xu, M.H. Zheng, K.R. Dai, Prevention of wear particle-induced osteolysis by a novel V-ATPase inhibitor saliphenylhalamide through inhibition of osteoclast bone resorption, PLoS One 7 (2012) e34132.
[12] M. Kogawa, K. Hisatake, G.J. Atkins, D.M. Findlay, Y. Enoki, T. Sato, P.C. Gray, Y. Kanesaki-Yatsuka, P.H. Anerson, S. Wada, The paired-box domain transcription factor Pax6 binds to the Upstream Region of the TRAP gene promoter and suppresses RANKL-induced osteoclast differentiation, J. Biol. Chem. 288 (2013) 31299–31312.
[13] W. Zou, T. Izawa, T. Zhu, J. Chappel, K. Otero, S.J. Monkley, D.R. Critchley, B.G. Petrich, A. Morozov, M.H. Ginsberg, Talin1 and Rap1 are critical for osteoclast function, Mol. Cell Biol. 33 (2013) 830–844.
[14] Z. Zhai, H. Li, G. Liu, X. Qu, B. Tian, W. Yan, Z. Lin, T. Tang, A. Qin, K. Dai, Andrographolide suppresses RANKL-induced osteoclastogenesis in vitro and prevents inflammatory bone loss in vivo, Br. J. Pharmacol. (2013), http://dx.doi.org/10.1111/bph.12463 [Epub ahead of print].
[15] H. Li, Z. Zhai, G. Liu, T. Tang, Z. Lin, M. Zheng, A. Qin, K. Dai, Sanguinarine Inhibits Osteoclast formation and Bone Resorption via suppressing RANKL-Induced Activation of NF-kappaB and ERK signaling pathways, Biochem. Biophys. Res. Commun. 430 (2013) 951–956.
[16] B. Tian, A. Qin, Z.Y. Shao, T. Jiang, Z.J. Zhai, H.W. Li, T.T. Tang, Q. Jiang, K.R. Dai, M.H. Zheng, Y.P. Yu, Z.A. Zhu, OA-4 inhibits osteoclast formation and bone resorption via suppressing RANKL induced P38 signaling pathway, Curr. Med. Chem. (2013) [Epub ahead of print].
[17] C. Wang, J.H. Steer, D.A. Joyce, K.H.M. Yip, M.H. Zheng, J. Xu, 12-O-tetradecanoylphorbol-13-acetate (TPA) inhibits osteoclastogenesis by suppressing RANKL-induced NF-κB activation, J. Bone Miner. Res. 18 (2003) 2159–2168.
[18] F. Ikeda, R. Nishimura, T. Matsubara, S. Tanaka, J.-I. Inoue, S.V. Reddy, K. Hata, K. Yamashita, T. Hiraga, T. Watanabe, Critical roles of c-Jun signaling in regulation of NFAT family and RANKL-regulated osteoclast differentiation, J. Clin. Invest. 114 (2004) 475–484.
[19] T.J. Weber, L.M. Markillie, Regulation of activator protein-1 by 8-iso-prostaglandin E2 in a thromboxane A2 receptor-dependent and-independent manner, Mol. Pharmacol. 63 (2003) 1075–1081.
[20] A. Qin, T.S. Cheng, Z. Lin, N.J. Pavlos, Q. Jiang, J. Xu, K.R. Dai, M.H. Zheng, Versatile roles of V-ATPases accessory subunit Ac45 in osteoclast formation and function, PLoS One 6 (2011) e27155.
[21] A. Qin, T. Cheng, N. Pavlos, Z. Lin, K. Dai, M. Zheng, V-ATPases in osteoclasts: Structure, function and potential inhibitors of bone resorption, Int. J. Biochem. Cell Biol. 44 (2012) 1422–1435.
[22] J.B. Moon, J.H. Kim, K. Kim, B.U. Youn, A. Ko, S.Y. Lee, N. Kim, Akt induces osteoclast differentiation through regulating the GSK3β/NFATc1 signaling cascade, J. Immunol. 188 (2012) 163–169.

[23] D.A. Stevenson, E. Schwarz, J.C. Carey, D.H. Viskochil, H. Hanson, S. Bauer, H.Y. Cindy Weng, T. Greene, K. Reinker, J. Swensen, Bone resorption in syndromes of the Ras/MAPK pathway, Clin. Genet. 80 (2011) 566–573.
[24] F. Ikeda, R. Nishimura, T. Matsubara, S. Tanaka, J. Inoue, S.V. Reddy, K. Hata, K. Yamashita, T. Hiraga, T. Watanabe, Critical roles of c-Jun signaling in regulation of NFAT family and RANKL-regulated osteoclast differentiation, J. Clin. Invest. 114 (2004) 475–484.
[25] A.E. Grigoriadis, Z.-Q. Wang, M.G. Cecchini, W. Hofstetter, R. Felix, H.A. Fleisch, E.F. Wagner, C-Fos: a key regulator of osteoclast-macrophage lineage determination and bone remodeling, Science 266 (1994) 443–448.
[26] H. Cao, K. Zhu, L. Qiu, S. Li, H. Niu, M. Hao, S. Yang, Z. Zhao, Y. Lai, J.L. Anderson, Critical of AKT in myeloma-induced osteoclast formation and osteolysis, J. Biol. Chem. 288 (2013) 30399–30410.
[27] A. Gingery, E.W. Bradley, L. Pederson, M. Ruan, N.J. Horwood, M.J. Oursler, TGF-β coordinately activates TAK1/MEK/AKT/NFkB and SMAD pathways to promote osteoclast survival, Exp. Cell Res. 314 (2008) 2725–2738.
[28] A. Gingery, E. Bradley, A. Shaw, M.J. Oursler, Phosphatidylinositol 3-kinase coordinately activates the MEK/ERK and AKT/NFkappaB pathways to maintain osteoclast survival, J. Cell Biochem. 89 (2003) 165–179.